

Design, Implementation and Experimental Validation of a DC-DC Resonant Converter for PEM Fuel Cell Applications

Maria Teresa Outeiro, Member IEEE
IPC/ISEC, Coimbra, Portugal
ISR, Porto, Portugal
touteiro@isec.pt, teresa.outeiro@fe.up.pt

Adriano Carvalho, Member IEEE
Department of Electrical and Computers Engineering
University of Porto, Portugal
asc@fe.up.pt

Abstract — When designing DC-DC resonant converters (RC) for PEM fuel cell applications some considerations must be fulfilled, such as; an appropriate topology, adequate control structure, accurate selection of the components namely, the power switches, heat sinks and core of each magnetic components and careful design of the HF transformer, resonant circuit and filters. The combination of all of these aspects defines the performance of the converter, hence the importance to be taken on its design. Particularly an accurate design of the RC defines its dynamics and stability. In this context, the paper is focused on the design, implementation and experimental validation of a DC-DC resonant converter for such applications. Once characterized the PEM fuel cell as electrical element of the circuit and defined the topology and control of the resonant converter its operation is analyzed based on second-order differential equation, where each one of the operation modes is treated separately. The constraints imposed by the PEM fuel cell are considered in the selection of the components, followed by the implementation of a 1kW prototype of the RC. The procedure proposed as well as the performance of the RC implemented in terms of dynamics and stability is validated by experimental results.

Keywords — fuel cell, series resonant converter, magnetic components design, HF transformer, prototype system.

NOMENCLATURE

PEM – Proton Exchange Membrane
VFC – Fuel cell voltage
IFC – Fuel cell current
A - Cell active area (cm²)
 λ - Membrane thickness (μm),
C - Equivalent capacitance (F)
B – Parameter dependent on cell type (V)
 $\zeta_1, 2, 3, 4$ ψ - Parametric coefficients (non dimensional)
J_{max} - Maximum current density (A/cm²)
RC – resonant converter
V_{out} – output voltage measured
V_{ref} – output voltage reference required
V_{error} – error of output voltage
f_s – switching frequency signals to the IGBTs
f_r – resonant frequency
Q - quality factor
I_{peak} - Peak current

I. INTRODUCTION

Nowadays, resonant conversion is widely used in meeting the strict specification norms of the power supplies [1-3], in electrical vehicles and battery chargers [4], induction-heating systems, high-voltage large current pulse charging sources, renewable energy sources like photovoltaic [5] and fuel cell systems [6;7], among others. Particularly, the DC power provided by a PEM fuel cell system that needs to be converted into utility interactive AC power requires a DC-DC boost converter to step-up their low DC voltage to peak the utility line voltage parameters. Such power converter consists typically of a DC-DC converter followed by a DC-AC converter as represented in Fig. 1. In order to reach the DC voltage level required for the AC-DC converter it is necessary to use a DC-DC boost converter, which, due to the large amplification requires galvanic isolation between the input, and the output. In this case a step-up transformer is normally used. In order to reduce the overall size, weight and cost of the converter as well as to achieve higher efficiency, high-frequency (HF) operation is recommended [6]. The switching losses can be mitigated by circuit topologies, which operate with soft switching to avoid both capacitive discharge and overlap of voltage and current at the switching instants. Many topologies of soft switching power conversion techniques have been investigated [8;9] particularly the use of Zero-Voltage Switching (ZVS) [10;11] and Zero-Current Switching (ZCS) [10;12;13] techniques are nowadays receiving renewed interest.

However, the design of a RC presents many challenges, among them the fact that it operates with frequency modulation instead of pulse-width modulation, requiring a different approach and design of the converter [14]. Then, once characterized the PEM fuel cell as electrical equivalent circuit and the resonant converter topology and control. Considerations on selecting the power switches, heat sinks, core of the magnetic components and on the design of the HF transformer, resonant circuit [7;14] and filters are presented. Finally, a 1kW prototype is implemented and tested to validate the dynamics and stability of the resonant converter proposed for the application.

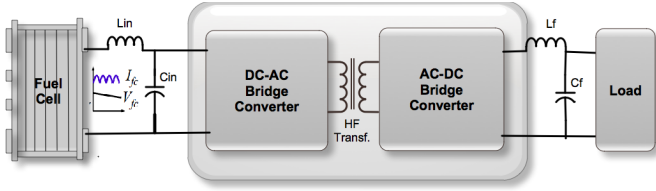


Fig. 1. Generic scheme of a DC-DC resonant converter.

II. PEM FUEL CELL

A PEM fuel cell is an electrochemical device that converts chemical energy from hydrogen, directly into heat, water and electrical energy. Similar to a battery, a fuel cell consists of two electrodes (anode and cathode) and an electrolyte as shown in Fig. 2.

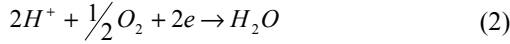
A. Operation

The electrochemical reactions involved inside the fuel cell stack can be described by (1) to (3) below.

Reaction in the anode side:



Reaction in the cathode side:



Overall reaction:



B. Electrical equivalent circuit of the PEM

The electrical equivalent circuit of Fig. 3 is adopted to analyze performance of the PEM fuel cell. This model is characterized by static and dynamic equations, which parameters need to be determined by nonlinear optimization algorithms such as SA.

The static behavior of the PEM fuel cell is represented in the model by a set of equations which parameter values are essential in the analysis of the performance. The output voltage of a single cell is defined by (4), where E_{Nernst} is the open voltage and the drops are due to the activation (V_{act}), ohmic (V_{ohmic}) and concentration (V_{con}) phenomena that occurs inside the cell.

$$V_{FC} = E_{Nernst} - V_{act} - V_{ohmic} - V_{con} \quad (4)$$

For n cells connected in series forming a stack, the output voltage V_s is defined by (5);

$$V_s = n \times V_{FC} \quad (5)$$

The dynamic behavior of the PEM is represented by the capacitor C and corresponds electrically to the phenomenon known as "charge double layer", on which the interface between electrode and electrolyte acts as storage of electrical charges and energy. This effect introduces a delay in the dissipation of electrical charges at the interface electrode/electrolyte, which affects the V_{act} and V_{con} terms, as shown by (7).

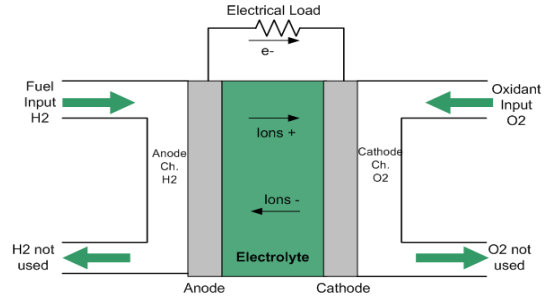


Fig. 2. Scheme of a single cell.

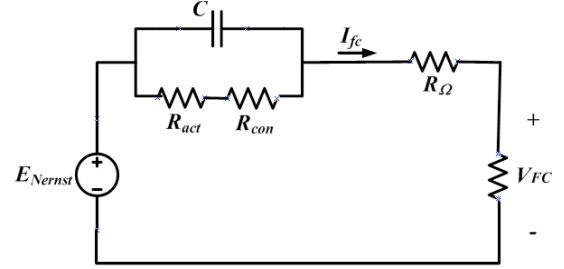


Fig. 3. Electrical equivalent circuit of the PEM.

$$\frac{dV_d}{dt} = \left(\frac{1}{C} \times i_{FC} \right) - \left(\frac{1}{\tau} \times V_d \right) \quad (6)$$

$$\tau = C \times R_a = C \times (R_{act} + R_{con}) = C \times \left(\frac{V_{act} + V_{con}}{i_{FC}} \right) \quad (7)$$

A set of parameters characterizes the electrical equivalent circuit adopted to analyze the performance of the PEM fuel cell: A - Cell active area (cm^2), λ - Membrane thickness (μm), RC - Contact resistance (Ω), C - Equivalent capacitance (F), B - Parameter dependent on cell type (V), $\zeta_1, 2, 3, 4$ and ψ - Parametric coefficients (non dimensional) and J_{max} - Maximum current density (A/cm^2).

III. RESONANT CONVERTER

A. Topology

The topology of the converter is represented in Fig. 4 and corresponds to a resonant series converter. Its operation can be described as follows: the voltage supplied by the fuel cell stack, which is typically low must be converted to a high and constant level, for example; 48 V or 400 VDC in order to be able to feed an electric vehicle or to be sent to the grid through an inverter. The HF transformer is a step-up voltage transformer, which also serves as galvanic isolation between the high and low voltage levels of the circuits. The waveforms of the voltage and current in the LC series resonant circuit in the primary side of the transformer are sinusoidal. Selecting appropriate values for the L_r and C_r components, the resonant frequency of the circuit is established. Then, the DC voltage of the fuel cell is firstly inverted in the primary side of the HF transformer, being rectified on the secondary side. The low pass filter in the primary side (L_{PEM}, C_{PEM}) allows at protecting the PEM fuel cell from the ripples of current and voltage produced by the converter, and also allows the storage of energy in the DC bus. The low pass filter in the secondary (L_f, C_f) allows at reducing the ripples of current and voltage to the load, respectively.

B. Control

The structure of control selected for the application is represented in Fig. 5. It combines two control loops; a fast loop, which is used to control the output voltage and a slow loop, which is used to move the operating point of the fuel cell to its optimum point in the polarization curve. The output voltage - V_{out} , is measured and compared to a reference voltage - V_{ref} , to generate an error signal - V_{error} . The PI controller, which is characterized by a fast dynamic response, takes care of the voltage error of the output voltage. The control of the operating point of the PEM fuel cell is accomplished by the slow loop, which is adapted to its characteristics.

C. Operation of the RC

The full bridge topology of Fig. 4 can be simplified to the equivalent circuit represented in Fig. 6, which corresponds to a 2nd-order differential equation where, V_{FC} is the PEM fuel cell, R_t and L_t are the transformer resistance and inductance parameters and R'_{load} is the load referred to the primary side of the transformer. This circuit has resonant frequency f_r (11) and impedance Z_r (12). For the operation of the converter below resonance with discontinuous current, a turn-on and a turn-off at ZCS conditions is obtained. This occurs when the tank presents a leading (capacitive) load to the switch network, which property allows natural commutation of the power switches and elimination of the switching losses.

1. Voltage

The output voltage of the full-bridge inverter is a square-waveform, wherein in the first half period $[0-\pi]$ the IGBTs Q1 and Q3 conduct and V_{FC} is positive, while in the second half period conduct IGBTs Q2 and Q4 $[\pi - 2\pi]$ and V_{FC} is negative accordingly to Fig. 4 and (8).

$$\begin{cases} +V_{FC}, & \text{for } 0 < \omega t \leq \pi \\ -V_{FC}, & \text{for } \pi < \omega t \leq 2\pi \end{cases} \quad (8)$$

2. Current

Similarly, the current is $i(t)$ is positive $+i(t)$ in the first half period $[0-\pi]$, and negative $-i(t)$, in the second half period $[\pi - 2\pi]$. Current $i(t)$ is well approximated by a sinusoid waveform as represented by (9) and (10).

$$i_{Q1} = i_{Q3} = \begin{cases} +Imax \times \sin(\omega t - \Phi), & \text{for } 0 < \omega t < \pi \\ 0, & \text{for } \pi < \omega t < 2\pi \end{cases} \quad (9)$$

$$i_{Q2} = i_{Q4} = \begin{cases} 0, & \text{for } 0 < \omega t < \pi \\ -Imax \times \sin(\omega t - \Phi), & \text{for } \pi < \omega t < 2\pi \end{cases} \quad (10)$$

If $XL_r = XC_r$ then $Z=R$ and the circuit operates at resonant conditions that is, for $f_s=f_r$, which is characterized by the resonant frequency f_r and characteristic impedance Z_r defined by (11) and (12).

$$f_r = \frac{1}{2\pi \times L_r C_r} \quad (11)$$

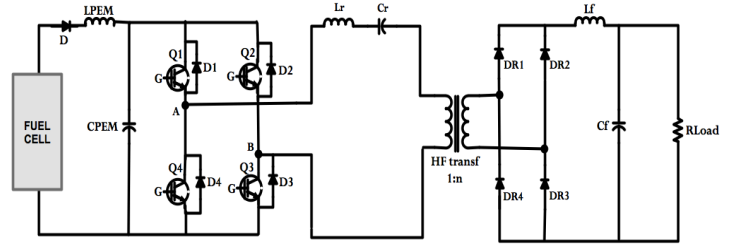


Fig. 4. Topology of the converter.

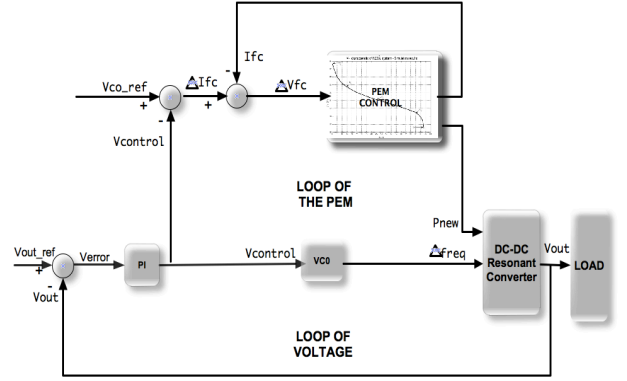


Fig. 5. Control of the converter.

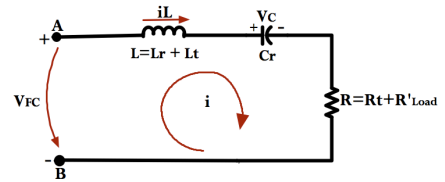


Fig. 6. Equivalent circuit of the converter.

$$Z_r = \sqrt{\frac{L_r}{C_r}} \quad (12)$$

3. Quality factor and Peak current

The quality factor Q , of a resonant circuit measures the "goodness" or quality of the circuit. A higher value of Q corresponds to a narrower bandwidth, which is desirable in many applications. More formally, Q is the ration of the power stored in the reactance to the power dissipated in the resistance of the resonant circuit. The quality factor is defined as:

$$Q = \frac{1}{R} \times \sqrt{\frac{L_r}{C_r}} \quad (13)$$

The peak current is defined by (14) and increases as the values of the input voltage and resonant capacitor increases and the value of resonant inductor decreases.

$$I_{peak} = Vin \times \sqrt{\frac{C_r}{L_r}} \quad (14)$$

The quality factor Q , defines de range or load that can be applied to the circuit and consequently, the power that can be transferred through this. Moreover, the power transferred depends of the peak current value in the circuit, the higher the current, the higher the amount of power is transferred.

IV. CONSIDERATIONS OF THE DESIGN

When designing a RC for any application, it is necessary to know the output specifications as well as the electrical and physical environment that the RC will operate in. In this session the design considerations are examined and the selection of resonant components (Lr, Cr), HF transformer and filters are made. The design considerations are performed for a PEM fuel cell of Ballard, the Mark1020, which constraints in voltage, current and power imposed to the converter are represented in the Table I. Only the minimum and maximum values achieved by experimental tests performed with the PEM Mark 1020 are considered.

A. Selection of resonant components

Two criteria are considered in the selection of the resonant components, Lr and Cr namely: 1st) Lr must be as low as possible and 2nd) Cr must be selected according to the power to transfer and operating frequency required by the control system. A third condition is considered in the present case, regarding the availability of capacitors at the lab.

Then, considering the minimum (19.11V) and maximum (23.71V) values of voltage provided by the PEM Mark1020, and the leakage inductance (2.1μH) value of the HF transformer, the maximum current in the resonant circuit (Imax_ress), maximum power transferred to the load (Pmax) and the output voltage level (Vout) achieved to the RC are presented in Table II for the two capacitors available in the lab, 4μF and 10μF. Table II shows that both, the maximum power transferred (Pmax) and the peak resonant current (Iress), increases with the capacitor value, Cr. Table II also shows that the output voltage (Vout) depends only of the input voltage level. Using the PEM Mark1020 to supply the converter, its output voltage can be regulated up to 234V. Accordingly to this analysis and considering the value of the leakage inductance of the transformer, the set of values selected for the resonant circuit are 2.1μH and 4μF as the resonant inductor and the capacitor respectively.

B. Resonant capacitor considerations

The resonant circuit requires a capacitor with higher operating voltages and ripple currents in order to support the need of increasing power. Accordingly, the important parameters that should characterize the resonant capacitor are; low inductance to limit the switching transient voltages, high frequency capability, large range of working temperature, long expected lifetime, high stability vs. time of the capacitance value, withstanding of high peak voltage, mechanical strength, low weight, maximum flexibility of adaptation to the shape of the available space and low total cost. The film capacitor is selected because this is the type of capacitor that comes closest to satisfying these requirements.

TABLE I. CONSTRAINTS IMPOSED BY THE PEM TO THE RC

I _{fc} (A)	V _{fc} (V)	Power (W)	Freq. Response
2.8	23.71	66	f < 1Hz
24	19.11	492	

TABLE II. PERFORMANCE OF THE RC FOR TWO CASE STUDIES

		VFC =19.11V	VFC =23.71V
Lr=2.1μH Cr=4μF	Pmax (W)	102.22	314.32
	Iress(A)	9.16	20.33
	Vout (V)	60.32	234.80
Lr=2.1μH Cr=10μF	Pmax (W)	340.03	487.59
	Iress(A)	26.58	31.82
	Vout (V)	60.4	234.76

C. Filters

The design of the PEM filter must be considered for the worst situation i.e., for which the fuel cell current is maximum and voltage minimum. A second consideration is related to the operating frequency of the converter, in which the worst situation is for its minimum; the filter cutoff frequency must be at least a decade below this one in order to smooth enough the fuel cell current.

The maximum current (Imax) of the resonant circuit appear in the DC side (i_{DC}) as follows.

$$i_{DC} = \frac{1}{\pi} \int_0^{\pi} I_{max} \sin(\omega t) d\omega t = \frac{2}{\pi} \times I_{max} \quad (15)$$

Considering a ripple of voltage of 2% of their nominal value (ΔVc) and the minimum frequency of the converter the inductor value and the capacitor value of filter can be calculated by (16) and (17).

$$i_c = C \frac{\Delta V_c}{\Delta t} \Leftrightarrow \Delta V_c = \frac{1}{C} \times \frac{2}{\pi} \times I_{max} \times \frac{1}{2 \times f_{conv}} \quad (16)$$

$$2\pi f_{filter} L = \frac{1}{2\pi f_{filter} C} \quad (17)$$

Hence, the LC components of the filters can be calculated by (18) and (19) respectively.

$$C = \frac{2}{\pi} \times I_{max} \times \frac{1}{2 \times f_{conv}} \times \frac{1}{\Delta V_c} \quad (18)$$

$$L = \frac{1}{(2\pi f_{filter})^2 \times C} \quad (19)$$

To protect the PEM Mark 1020 of voltage and current ripples, the components of the low pass filter selected and implemented experimentally are: C_{PEM} = 940 μF, and L_{PEM} = 933 μH, corresponding to a cutting frequency of 170 Hz. Similarly to the PEM filter, the output filter components selected are C_{out} = 110 μF and L_{out} = 536 μH, corresponding to a cutting frequency of 557 Hz.

D. HF transformer

The main goal of the HF transformer beyond power transfer is to provide the isolation between low and high voltages and to raise the voltage of the converter. The physical size of the HF transformer is dependent on the power to be transferred as well as on the operating frequency. At high frequency operation the size is smaller. If the converter operates with a switching frequency closed to the resonant frequency f_r , the maximum transfer of power to the load occurs. The design of the transformer also depends of the value of the input voltage, which determines the turn's number and wire-diameter of 1° and 2° windings. Thus the first step in designing the HF transformer is to choose the appropriate core to use, for instance the ferrite type EE of N27 material is a good option to use as the core material for the case. The main characteristics of the HF transformer implemented in the lab are presented in Table III.

V. EXPERIMENTAL IMPLEMENTATION AND VALIDATION

The experimental prototype of the converter is shown in Fig. 7. In this figure it can be observed the various analog control boards implemented as well as the power supply of $\pm 15V$ for the control circuit. The power circuit, which is composed by two full bridges, inverter and rectifier, HF transformer and filters, ensures the transfer of the power of the PEM to the load. With a resonant frequency (f_r) defined to 33kHz, the converter operates in discontinuous conduction mode by controlling its resonant power pulses frequency (f_s) in the range of $f_s < f_r$, which maximum frequency is the resonant (f_r) and the minimum frequency is set to 1900Hz.

In order to validate the design procedure proposed and to analyze the performance of the RC in terms of dynamics and stability, some experimental results are presented and discussed in this section, namely; the PI and Vcontrol signals, the IGBT signals, and the output voltage and currents in the converter.

A. Controller

The actions performed by the controller to a step-down of load are shown in Fig. 8. Accordingly to the control structure presented in Fig. 5, the faster loop of the controller is responsible to keep the output voltage of the converter in a constant value, therefore the PI controller reacts accordingly and the Vcontrol signal is sent to the VCO to meet the goal i.e. to keep the output voltage in the reference predefined by the user, minimizing the error of voltage. Accordingly, the Vcontrol signal is sent to the oscillator, which in turns leads, the converter to change its operating frequency in accordance to the load level requested. In the case of a step-down load level, the Vcontrol signal is lowered and consequently the operating frequency decreases while the output voltage remains constant. The signals that are sent to the gates of IGBTs 1 and 3 are in opposition to the signals sent to the IGBTs 2 and 4 as can be observed in Fig. 9. A dead time is visible between the impulses sent to the same branch of the inverter bridge, which must be ensured in order to avoid short circuits. The dead time between the impulses is of $4\mu s$ for the case.

TABLE III. HF TRANSFORMER PARAMETERS

N1	N2	Core	Rt	Lt	RM	LM
2	20	Ferrite EE	0.18	2.1E-6	286	9.2E-4

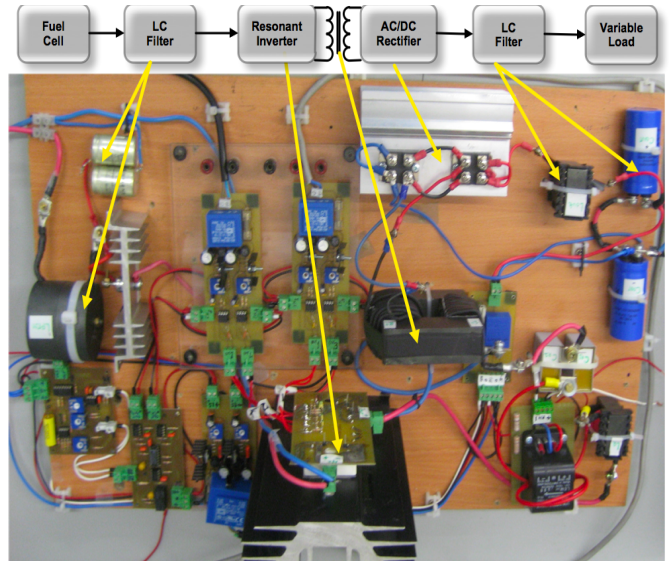


Fig. 7. Prototype of the converter.

B. Dynamics and Stability of the converter

As is observed in Fig. 10, the converter reacts to a load variation, varying its frequency accordingly ensuring a correct operation of the converter and transfer of the power from the PEM to the load. The operating frequency varies instantaneous with the variation of load; hence it can be concluded that the control system presents a good dynamics.

From Fig. 11 it is observed that the output voltage remains constant despite the load variation ensuring a good stability of the converter system.

Both the characteristics of dynamics and stability previously demonstrated for the condition of step-down of load requested are also valid for the condition of step-up of load. These are assured by the inner loop or control of the voltage. The outer loop or loop of the PEM is not analysed in this paper.

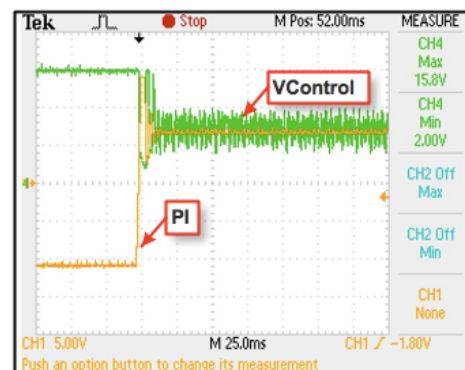


Fig. 8. Response of PI and Vcontrol signals to a step-down of the load.

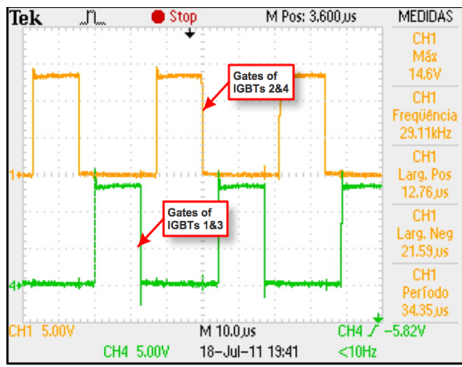


Fig. 9. Gate drive signals sent to the gates of the IGBTs.

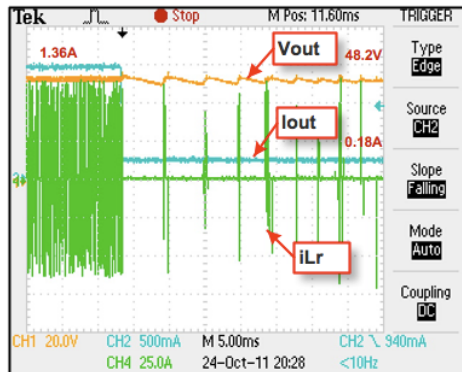


Fig. 10. Response of the converter to a step-down of load.

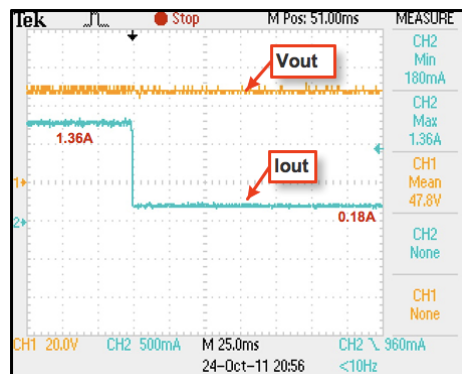


Fig. 11. Stability of the system to a step-down of the load.

VI. CONCLUSIONS

A proposal of designing a DC-DC resonant converter for PEM fuel cell applications is presented. Due to the advantages associated to resonant conversion, namely the optimization of the switching losses this technique is selected. So it is appropriate to operate the converter at higher frequency in order to reduce size and weight of the magnetic components as well as of filtering components.

Once selected the topology and the control for the converter and analyzed its operation, considerations on designing HF

transformer, resonant tank components and filters are presented.

The steady-state operation of the converter is validated based on a prototype of 1kW and the dynamics making use of step change of the load. From experimental results it is observed that the converter controller shows a very good dynamics performance, demonstrating robust stability..

So, within the frame of converting a fuel cell in a voltage controlled power source the paper presents the design process of fuel cells based systems validated with performance characteristics shown with a prototype.

REFERENCES

- [1] T.W. Ching, K.U.Chan "Review of Soft-Switching Techniques for High-Frequency Switched-Mode Power Converters". in IEEE Vehicle Power and Propulsion Conference (VPPC). 2008. Harbin, China.
- [2] N. Shafiee, M. Pahlevaninezhad, H. Farzanehfard, A. Bakhshai, P. Jain, "Analysis of a Fifth-Order Resonant Converter for High-Voltage DC Power Supplies". IEEE Transactions on Power Electronics, 2013. 28(1): pp. 85 - 100.
- [3] H. Babu Kotte, R.A., K. Bertilsson, "High-Speed (MHz) Series Resonant Converter (SRC) Using Multilayered Coreless Printed Circuit Board (PCB) Step-Down Power Transformer". IEEE Transactions on Power Electronics, 2013. 28(3): pp. 1253 - 1264.
- [4] B. Gu, J.-S.Lai, N. Kees, C. Zheng, "Hybrid-Switching Full-Bridge DC-DC Converter With Minimal Voltage Stress of Bridge Rectifier, Reduced Circulating Losses, and Filter Requirement for Electric Vehicle Battery Chargers". IEEE Transactions on Power Electronics 2013. 28(3): p. 1132 - 1144.
- [5] O. Mostaghimi, N.Wright, A. Horsfall, "Design and Performance Evaluation of SiC Based DC-DC Converters for PV Applications", in 4th Annual IEEE Energy Conversion Conference and Exposition. 2012: Raleigh, North Carolina. pp. 3956 - 3963
- [6] A. Andreiciks, I. Steiks, O. Krievs, "Design of Resonant DC/DC Converter for Fuel Cell Application", in 13th Biennial Baltic Electronics Conference (BEC2012). 2012: Tallinn, Estonia. pp. 219 - 222.
- [7] Y. Nishida, S. Sumiyoshi, H.Omori, "Integrated power converter for photovoltaic and Fuel Cell systems in home", in 13th Power Electronics and Motion Control Conference EPE-PEMC. 2008: Poznań, Poland. pp. 2530 - 2537.
- [8] A. Rathore, A. Bhat, R. Oruganti, "A Comparison of Soft-Switched DC-DC Converters for Fuel Cell to Utility Interface Application". IEEE Proceedings, 2007: pp. 588-594.
- [9] O. Krykunov, "Comparison of the DC/DC-Converters for Fuel Cell Applications". International Journal of Electrical, Computer, and Systems Engineering, 2007. 1(1): pp. 71-79.
- [10] D.C. Hamill, K.N. Bateson, "Design oriented analysis of a resonant ZVS/ZCS DC-DC converter". Fifth European Conference on Power Electronics and Applications, 1993. 3: pp. 23-29.
- [11] F.Z. Peng, H. Li, Gui-Jia Su, J.S. Lawler, "A New ZVS Bidirectional DC-DC Converter for Fuel Cell and Battery Application". IEEE Transactions on Power Electronics, 2004. 19(1): pp. 54-65.
- [12] Y.-S. Lee, Y.-Y. Chiu, M.-W. Cheng, "Inverting ZCS Switched-Capacitor Bi-directional Converter", in 37th IEEE Power Electronics Specialists Conference, PESC'06. 2006: Jeju, Korea.
- [13] H. Pollock, J.O. Flower, "New Method of Power Control for Series-Parallel Load-Resonant Converters Maintaining Zero-Current". IEEE Transactions on power electronics. 1997. 12(1): pp. 103-115.
- [14] B. Lin, C.Chao, "Analysis, Design, and Implementation of a Soft-Switching Converter With Two Three-Level PWM Circuits". IEEE Transactions On Power Electronics, 2013. 28(4): pp. 1700 - 1711.